

New long-wavelength ethanolamino-substituted hypocrellin: photodynamic activity and toxicity to MGC803 cancer cell

Hua-Yang Lee^a, Zhi-Xiang Zhou^b, Shen Chen^a, Man-Hua Zhang^{a,*}, Tao Shen^a

^aKey Laboratory of Photochemistry, Center for Molecular Science, Institute of Chemistry, Chinese Academy of Sciences, Beijing 100080, PR China

^bInstitute of Biophysics, Chinese Academy of Sciences, Beijing 100101, PR China

Received 20 February 2004; received in revised form 16 May 2004; accepted 23 June 2004

Available online 5 March 2005

Abstract

To improve hydrophilicity and photoactivity of the new type of therapeutic agent, hypocrellin, a novel long-wavelength ethanolamino-substituted hypocrellin B (EAHB) was synthesized and its molecular structure was characterized by IR, NMR, MS, and UV–vis spectrometers, and EAHB had strong absorption at the phototherapeutic window (600–900 nm). Illumination of deoxygenated DMSO solution containing EAHB generated a strong electron paramagnetic resonance (EPR) signal, which was assigned to the semiquinone anion radical of EAHB (EAHB^{•-}). Absorption measurements displayed that the absorptive bands at 632 and 565 nm (shoulder) arose from the semiquinone anion radical (EAHB^{•-}) and the absorptive bands at 519 and 450 nm (shoulder) belonged to hydroquinone (EAHBH₂), which were formed via the decay of EAHB^{•-} in water-contained solution. Superoxide anion radical (O₂^{•-}) was produced via electron transfer from EAHB^{•-} (the precursor) to ground state oxygen. The presence of NADH, a bio-electron donor, significantly enhanced production of EAHB^{•-} and O₂^{•-}. Singlet oxygen O₂(¹Δ_g) could be produced via energy transfer from triplet EAHB to ground state oxygen molecules. The quantum yield of O₂(¹Δ_g) and the relative quantum yield of O₂^{•-} of EAHB were 0.15 and 0.76, respectively, with the parent compound hypocrellin B (HB) as the standard. It was inferred that Type I pathway was possibly a major photodynamic mechanism of EAHB. The study on photobiological action of EAHB on MGC803 cancer cells revealed that EAHB kept the same good phototoxic ability as HB but reduced 4 times cytotoxicity than HB, and also its photopotential factor increased 4-folds.

© 2005 Elsevier Ltd. All rights reserved.

Keywords: Ethanolamino-substituted hypocrellin B; EPR spectra; Phototoxicity; Singlet oxygen; Superoxide anion radical

1. Introduction

Photodynamic therapy (PDT) is a promising new treatment for light-accessible tumors [1,2], which is a multi-modality method requiring both a selective photosensitizer and a powerful light source that matches

the absorption spectrum of the photosensitizer. The initial photochemical process leading to the death of tumor cell may follow two principal pathways: (A) it engages in electron and proton transfer reaction with biomolecules to produce active free radical (Type I), alternatively, (B) upon light absorption, the photosensitizer transfers the energy to oxygen to yield singlet oxygen (Type II). Either pathway will require oxygen to propagate active species via radical chain reaction [3,4]. Under extensive and intensive investigations for the past

* Corresponding author. Fax: +86 10 82617315.

E-mail address: tshen@infoc3.icas.ac.cn (M.-H. Zhang).

two decades, hypocrellins, natural perylenequinoid pigments, are potential photosensitizers for PDT treatment to tumor cells through the damage mechanisms of Type I and II mentioned above [5]. Recently, hypocrellins have been reported to display photoinduced antiviral activities against the human immunodeficiency virus (HIV-1), herpes simplex virus via Type I, Sindbi virus, and vesicular stomatitis virus (VSV) with the Type II mechanism [6–8]. Moreover, the PDT effectiveness of hypocrellins is reported relative to the proton transfer of their excited state and intracellular pH decrease in 3T3 cells just like hypericin [9,10]. He et al. reported pK_a of HB at the excited state is lower than at ground state, which is important to antiviral and antitumor activity [11]. The proton transfer ability depends on the intramolecular hydrogen bond structure of 4,9-dihydroxy-3,10-perylenequinone moiety, and if the original peri-hydroxylated perylenequinone structure is modified by the amino substitution, the intramolecular liable proton transfer process is impeded which causes a reduced antitumor activity [12].

Furthermore, hypocrellins are insoluble in water and do not exhibit strong absorption in the domain of the phototherapeutic window (600–900 nm); these disadvantages limit their application in clinical treatments. Since 1996, some prospective amino-substituted hypocrellin derivatives have been synthesized. They possess much stronger absorption in the therapeutic window, good phototoxicity to tumor cells and higher photodynamic activities [13–15], but their poor hydrophilicity was still not conducive to their application in clinical treatments [16]. Although the mechanism of photosensitizer retention by tumor is not well understood, the balance between lipophilicity and hydrophilicity is recognized as a key factor influencing the photodynamic effectiveness and tumor cell uptake [17]. Hoping to obtain some kind of new compound with improved polarity and hydrophilicity of hypocrellin B and to keep the advantages of amino-substituted hypocrellin derivatives, we selected ethanolamine to further modify the structure of HB and obtained a new compound of 2-ethanolamino-2-demethoxy-17-ethanolimino-hypocrellin B Schiff base (EAHB) which still remains the structure of peri-hydroxylated perylenequinone.

The semiquinone anion radical of hypocrellin was considered to be a key intermediate in the cytotoxic reaction with the ability to generate toxic species such as $O_2^{\cdot-}$ in the presence of oxygen or directly react with the substrates in the absence of oxygen. The hydroquinone might also play an important role in the cytotoxic reaction, since it can be oxidized to generate semiquinone anion radical and active oxygen species through an electron transfer [18–20]. Wu et al. has reported the photodynamic action of 2-butylamino-2-demethoxy-hypocrellin (BAHB) [14]; there existed both Type I and II mechanisms, but the Type I mechanism was the major

process during its photoinduced damage to cancer cells, which is further proved by thermodynamic calculation [14,16]. BAHB has shown excellent phototoxicity to tumor cells, such as HeLa cancer cell, murine ascitic hepatoma cells and human pancreatic cancer cell line Capan-1 cells and low cytotoxicity to normal tissue cells [14–16]. Similarly, as a potential phototherapeutic agent with amino group, it is important to investigate the photodynamic mechanism and efficiency of EAHB and its potential photobiological anti-cancer ability. In this paper, we will emphasize on reporting the generation of semiquinone anion radical, superoxide anion radical, and singlet oxygen altogether during the photosensitization of this new photosensitizer by electronic paramagnetic resonance (EPR) and spectrophotometer measurements; we will discuss the formation mechanism of semiquinone anion radical, superoxide anion radical in presence of bio-electronic and proton donor NADH. Meanwhile, the corresponding MGC803 cancer cellular experiments compared with HB have been carried out to examine its phototoxicity, cytotoxicity and photopotential factor.

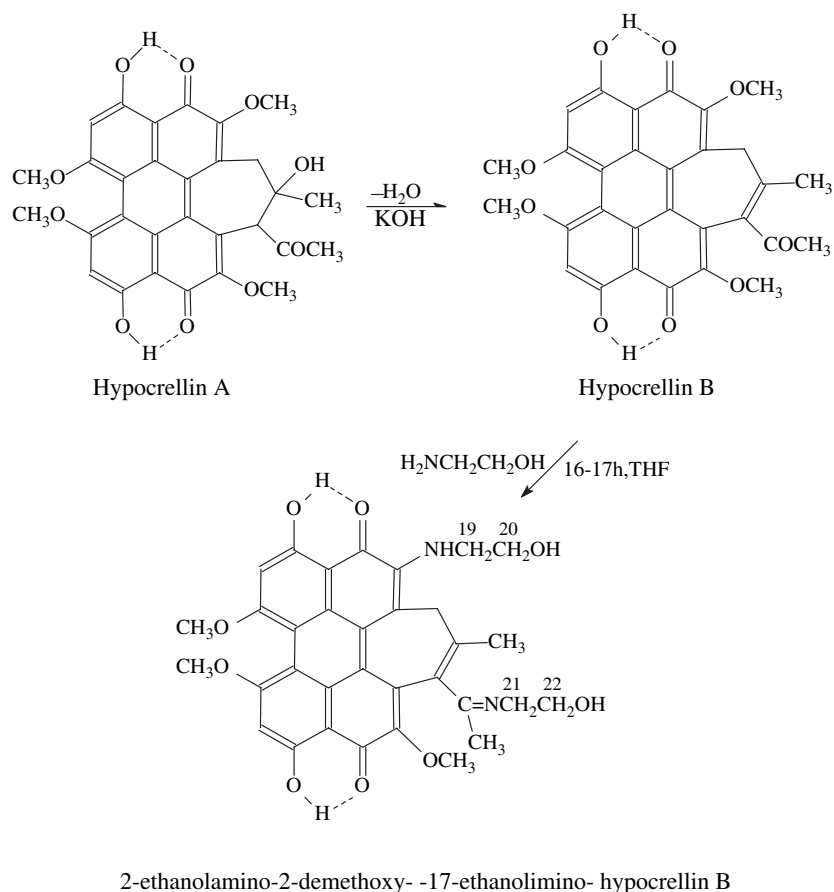
2. Materials and methods

2.1. Chemicals

HB was prepared by dehydration of HA in alkaline solution and purified by recrystallization twice from acetone [21] (Scheme 1). 2,2,6,6-Tetramethyl-4-piperidone (TEMP), 5,5-dimethyl-1-pyrroline-*N*-oxide (DMPO), nicotinamide adenine dinucleotide tetrahydrate (NADH), *p*-benzoquinone (PQ), 9,10-diphenyl-anthracene (DPA) and 1,4-diazabicyclo-(2,2,2)-octane (DABCO) were purchased from Aldrich, USA. Ethanolamine (A.R.), tetrahydrofuran (THF) and other solvents were purchased from Beijing Chemical Plant, China, and further purified before use.

2.2. Preparation of EAHB

HB (200 mg, powder, stored in the dark) was dissolved in fresh distilled THF (150 ml) containing reduced-pressure distilled ethanolamine (15 ml). The solution was stirred in the flask for 16–18 h at 50–55 °C in the dark. THF was evaporated under reduced pressure. And the remainder was dissolved in chloroform, and washed with 2–5% potassium dihydrogen phosphate solution ($CHCl_3:H_2O = 5:1$ v/v) several times until the pH of water layer was neutral. The chloroform layer was concentrated and the chloroform was removed to afford a black solid residue. And then the mixture was separated by TLC on a 1% potassium dihydrogen phosphate silicon gel plate, using 5:4 (v/v) acetone/cyclohexane as eluent, and



Scheme 1. The structures of hypocrellin A, B and the new derivative and the conversion between them.

2-ethanolamino-2-demethoxy-hypocrellin B Schiff base (EAHB: 14 mg, 7%; R_f 0.43, azure) was obtained (in contrast, HB R_f 0.94, red) with purity 98%. The structure of EAHB was identified on the basis of the UV–vis, IR, ^1H NMR and MS spectroscopic data (Scheme 1).

2.3. Measurements

2.3.1. Spectrometer measurement

Ultraviolet–visible (UV–vis) absorption spectra were recorded on a Shimadzu UV-160-A spectrometer. Infrared spectra (IR) were measured on a Perkin–Elmer 557 grating spectrometer. Mass spectra (MS) were conducted on a MALDI-TOF MS of Bruker BIFLEX III spectrometer and proton nuclear magnetic resonance (^1H NMR) spectra were recorded on a Varian XL-300 spectrophotometer in deuterated chloroform with TMS as internal standard. EPR spectra were measured on an ESR 300E spectrometer.

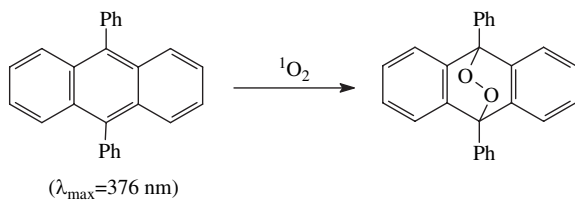
2.3.2. Determination of active oxygen species generation

Electron paramagnetic resonance (EPR) spectra were recorded on a Bruker Model ESR 300E spectrometer at room temperature. Samples were introduced into the

specially made quartz cup and illuminated directly inside the microwave cavity. All samples were purged with purified O_2 for 30 min in the dark and irradiated directly in the cavity of EPR spectrometer with Q-switched Nd:YAG nanosecond laser apparatus (full width at half-maximum, 35 mJ/pulse; $\lambda = 532$ nm).

The EPR measurement of spin trapping by TEMP was used to determine the generation of singlet oxygen by the photosensitizer. The reaction solution consisted of 0.1 mM photosensitizer and 20 mM TEMP [21]. The DPA bleaching method confirmed the quantum yields of singlet oxygen generation [22]. A solution of sample mixed photosensitizer and DPA (a singlet acceptor) was irradiated at a selected irradiation wavelength (560 nm), which was absorbed only by the photosensitizer; the reaction was followed spectrometrically by observing the decrease in the 374 nm absorption peak of DPA as a function of irradiation time (Scheme 2), where the photosensitizer has the smallest absorption.

The EPR measurement of spin trapping by DMPO was used to determine the generation of superoxide anion radical ($\text{O}_2^{\cdot-}$) by the photosensitizer similar to the method of determining the generation of singlet oxygen by the photosensitizer. The reaction solution consisted of 0.2 mM photosensitizer and 40 mM DMPO.



Scheme 2. The photooxidation of 9,10-DPA to its endoperoxide derivative by singlet oxygen.

2.3.3. Determination of semiquinone radical anion and effect of electron donor

Irradiation of EAHB (1 mM) in an argon-gassed dimethylsulphoxide (DMSO) solution for 1 min led to the generation of a strong ESR signal. The productions of the semiquinone anion radical and hydroquinone in a deoxygenated DMSO–buffer (1:1 by volume, pH = 8.0) solution containing EAHB (40 μM) solution with an electronic donor NADH (1 mM) were measured by the variances of absorbance between 400 and 700 nm on a Shimadzu UV-160-A spectrometer, through photolysis experiments according to the method of Hu et al. [23].

2.3.4. Cell survival studies

MGC803 cancer cells were presented by the Institute of Biophysics, Chinese Academy of Sciences. The cells were cultured in RPMI 1640 medium supplemented with 5% fetal bovine serum (FBS), 100 $\mu\text{g}/\text{ml}$ of penicillin, 100 $\mu\text{g}/\text{ml}$ of streptomycin at 37 $^{\circ}\text{C}$ in a Forma Scientific water-jacketed 5% carbon dioxide incubator.

Exponentially growing cells in 35 mm dishes (NUC) were incubated with increasing concentrations of photosensitizer from 0 to 16 μM in RPMI 1640 medium (FBS-free) for 4 h. The cells were irradiated with light dose of 8 J/cm^2 . The control group contained cells without laser treatment with increasing concentrations of photosensitizer from 0 to 200 μM . A second group of controls underwent treatment with a red light therapy without addition of photosensitizer. The light source was a Red light Treatment Instrument (Institute of Electronics, Academia Sinica China); its total power output was more 90% at 600–700 nm. After irradiation, the cells were placed in RPMI 1640 medium containing 5% FBS and incubated for 24 h before survival assessment. Cells survival was estimated by the MTT assay [24,25].

3. Results and discussion

3.1. Preparation and structural appraisal of new HB derivative

The ethanolamination of HB can afford EAHB, only being carried out in the solvent of THF or in the

water–THF mixed solution. Compared with HB, the much lower R_f values of EAHB in the silica TLC indicated that the hydrophilicity and polarity of it were much more improved than those of HB (EAHB: R_f 0.43, azure; HB: R_f 0.94, red in contrast). The compound keeps the original peri-hydroxylated perlenequinone structure of the parent pigment, the role of labile protons is important in the photodynamic treatment [26].

Ethanolamination of HB in THF afforded the aminated hypocrellin of EAHB (Scheme 1). Based on the UV, IR, ^1H NMR and MS data, the ethanolaminated hypocrellin was identified to be 2-ethanolamino-2-demethoxy-17-ethanolimino-hypocrellin B Schiff base:

TOF MS (M^+ , 600); IR cm^{-1} (KBr, ν_{\max}): 3427, 2925, 2854, 1610; UV–vis: ($[\text{CDCl}_3]$ λ_{\max} , nm [$\log \epsilon$]): 477 (3.68), 629 (4.03); ^1H NMR (300 MHz, CDCl_3) δ (ppm) 1.55 (3H, s, CH_3 -16), 2.20 (3H, s, CH_3 -18), 2.65 (1H, d, H-13a, $J_{\text{AB}} = 11.5$), 2.5–3.4 (3H, m, broad, HOCH_2 -20, HOCH_2 -22 and $-\text{NHC}$ -2), 3.63 (2H, m, NHCH_2 -19), 3.67 (1H, d, H-13b, $J_{\text{AB}} = 11.5$), 3.78 (2H, m, $=\text{NCH}_2$ -21), 3.83 (2H, m, HOCH_2 -22), 3.92 (2H, m, HOCH_2 -20) 4.05 (3H, s, OCH_3 -7), 4.06 (3H, s, OCH_3 -6), 4.20 (3H, s, OCH_3 -11), 6.20 (1H, s, H-5 (8)), 6.93 (1H, s, H-8(5)), 13.10 (1H, OH-9(10)), 16.40 (1H, OH-3(4)).

3.2. Absorption spectra of the derivative

The absorption spectra of EAHB are shown in Fig. 1. Based on the study of absorption spectra of HB [27], the shorter wavelength absorption band at 477 nm was assigned to the π – π^* transition and the absorption of the longer wavelength at 629 nm was in relation to intramolecular charge transfer (ICT) (seen from Fig. 1), which may take on some active role in the photodynamic activity. Compared with HB, the absorption at longer wavelength of EAHB was enhanced obviously, judged from Fig. 1, the molar absorption coefficients at

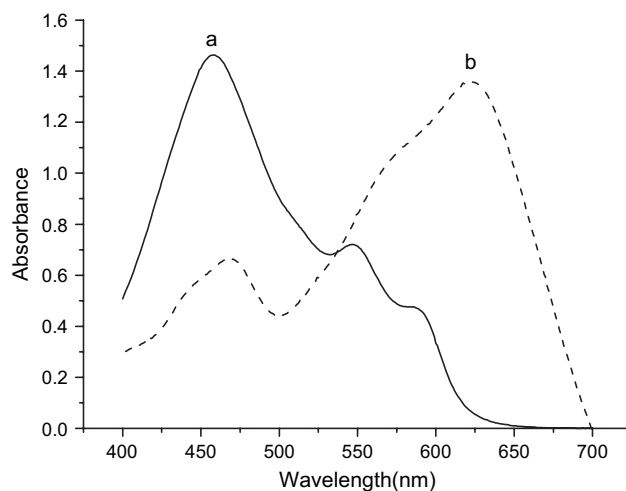


Fig. 1. Absorption spectra of a: HB (50 μM), b: EAHB (50 μM) in chloroform solution.

650 nm for the new derivative, EAHB was $\log \varepsilon = 3.91$ while the parent compound HB exhibits little absorption at 650 nm. EAHB has the maximum absorption around 580–630 nm in CHCl_3 (EAHB: $\lambda_{\text{max}} = 629$ nm, $\log \varepsilon = 4.03$), while the parent compound HB has relatively weak absorption (HB: $\lambda_{\text{max}} = 580$ nm, $\log \varepsilon = 3.52$). The absorption spectra of the new derivative red-shift distinctly and extend photoresponse into the photodynamic window (600–900 nm), which is important for the PDT.

3.3. Generation of semiquinone radical anion, superoxide anion radical $\text{O}_2^{\cdot-}$ and $\text{O}_2(^1\Delta_g)$ during the photosensitization of EAHB

3.3.1. Photogeneration of semiquinone radical anion and effect of electron donor

Irradiation of EAHB (1 mM) in an argon-gassed dimethylsulphoxide (DMSO) solution for 1 min led to the generation of an ESR signal as shown in Fig. 2A,

with $g = 2.0036$. The structure of this EPR spectrum was very similar to that of the semiquinone radical anion of HB [28]. The intensity of the signal increased rapidly during photoirradiation and decreased very slowly in the dark. The ESR signal intensity of EAHB radical depended on the presence of oxygen, which quenched the ESR signal (Fig. 2B). But if the concentration of EAHB was higher (10 mM) and the illumination time was long enough (> 4 min), the signal can still be detected even in the aerated DMSO solution. The ESR spectrum observed may be ascribed to the semiquinone radical anion of EAHB ($\text{EAHB}^{\cdot-}$). The concentration effect indicated that $\text{EAHB}^{\cdot-}$ radical might be generated by self-electron transfer between the ground and the excited states [29]:



The radical cation of semiquinone is very difficult to be detected in common organic solvents and water,

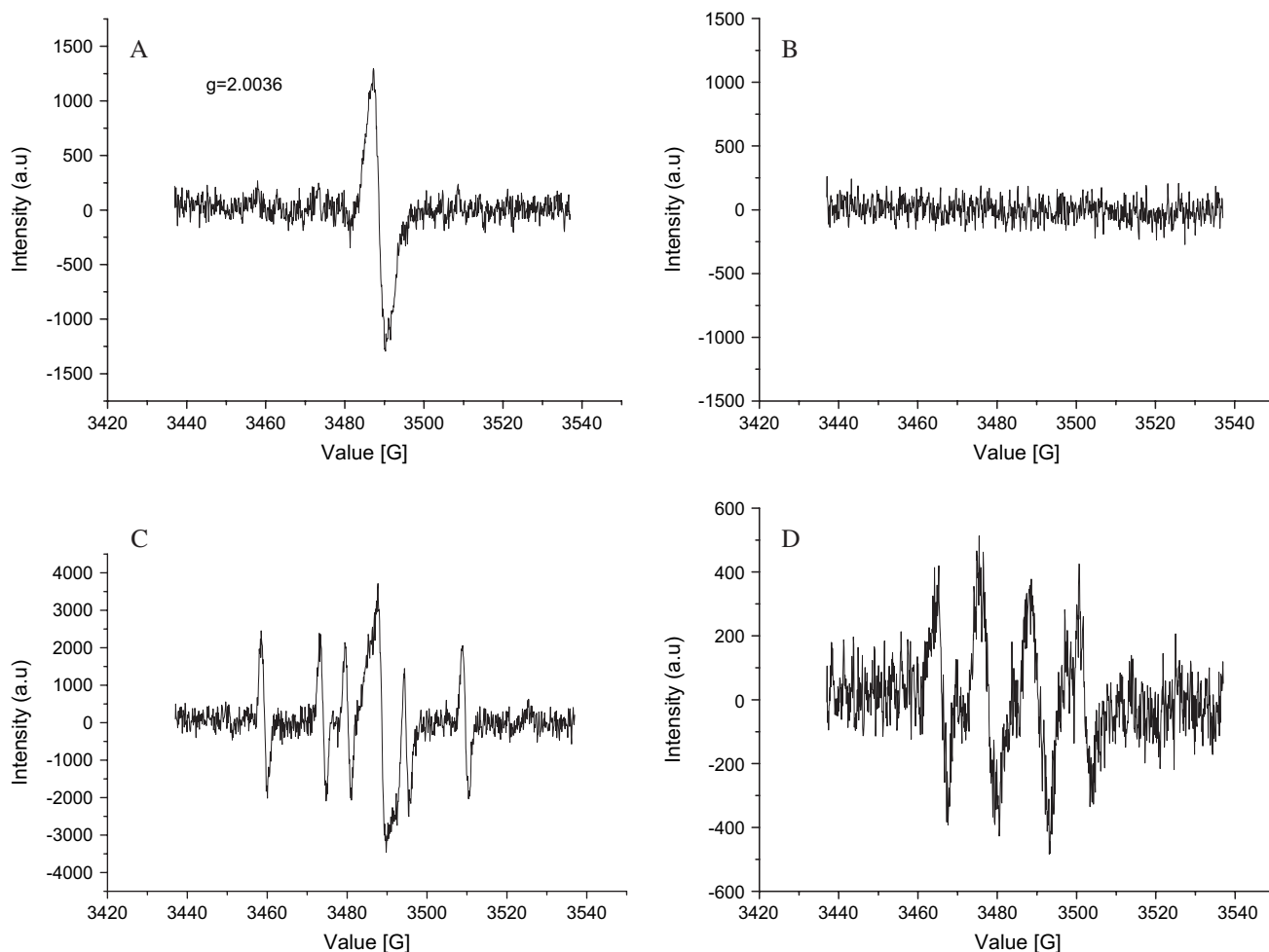
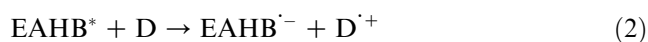


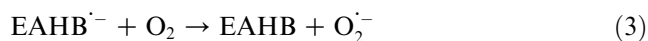
Fig. 2. (A) EPR spectrum from a deaerated DMSO solution of EAHB (1 mM) on the irradiative at 532 nm for 1 min; (B) same as spectrum A, but oxygen was bubbled through the solution before illumination; (C) same as spectrum A, but in the presence of NADH (1 mM) and DMPO (20 mM), irradiation for 1 min; and (D) same as spectrum A, but in the presence of DMPO (20 mM) and oxygen was bubbled through the solution after irradiation for 1 min. Instrument setting: microwave power, 1 mW; modulation amplitude, 1.012 G; time constant, 0.1024 s.

owing to its strong oxidizing ability [30]. In order to identify this deduction, the sample of EAHB (1 mM) in DMSO was illuminated for 1 min, in the presence of a typical bio-reductant, NADH and a spin trapper, DMPO. The ESR signal of EAHB^{•-} with an apparent DMPO-CH₃ signal ($\alpha^N = 16$ G, $\alpha^H = 22.8$ G) [31] was intensified significantly (Fig. 2C). Moreover, in the presence of other reductants such as EDTA, BNAH and cysteine, the EPR signal of EAHB^{•-} was also intensified. These phenomena indicated the anionic character of the radical, EAHB^{•-}, in the presence of electron donor (D) may be generated by the following:



The appearance of DMPO-CH₃ may result from NADH^{•+} attacking the DMSO solvent molecule and [•]CH₃ is captured by DMPO. It must be emphasized that EAHB^{•-} was also formed under aerobic conditions but was not obviously observed due to the rapid reaction with O₂^{•-}, when irradiating EAHB (1 mM) in an oxygen-gassed DMSO solution with O₂^{•-} spin trapper of DMPO (20 mM) for 30 s led to the generation of an ESR signal as shown in Fig. 2D, the signal of semiquinone radical anion of EAHB disappears gradually, and the signal of DMPO-OOH is observed with a 12-line EPR spectrum [32].

The formation of O₂^{•-} is the result of the interaction between EAHB^{•-} and ground state oxygen. In addition, the O₂^{•-} signal can be observed only in a polar solvent such as DMSO or DMF; and there is no apparent O₂^{•-} signal appearing in chloroform, cyclohexane, or other non-polar solvents. Results being described above indicate a major Type I reaction mechanism was involved.



Absorptive spectra measurements on the deoxygenated DMSO–buffer solution containing EAHB and NADH also confirmed that the Type I mechanism was involved in the photosensitization process. The absorption maxima of EAHB in DMSO–buffer (1:1 by volume) solution are at 475 and 632 nm for pH = 8.0, owing to the dissociation of the phenolic hydroxyl groups in the chromophore of hypocrellin. The color of the sample (pH = 8.0) containing EAHB and electronic donor underwent the changes from azure (the color of the EAHB) to yellowish green and then to orange, on photoinduced reduction of EAHB in weak alkaline media: deoxygenated DMSO–buffer (1:1 by volume, pH = 8.0) solution containing EAHB (40 μM) and NADH (1 mM) (i.e. in pH = 5 or 11, we did not observe the above apparent photoinduced reduction of EAHB). Fig. 3 shows the absorption curves recorded during the irradiation: (A) The height of the absorption

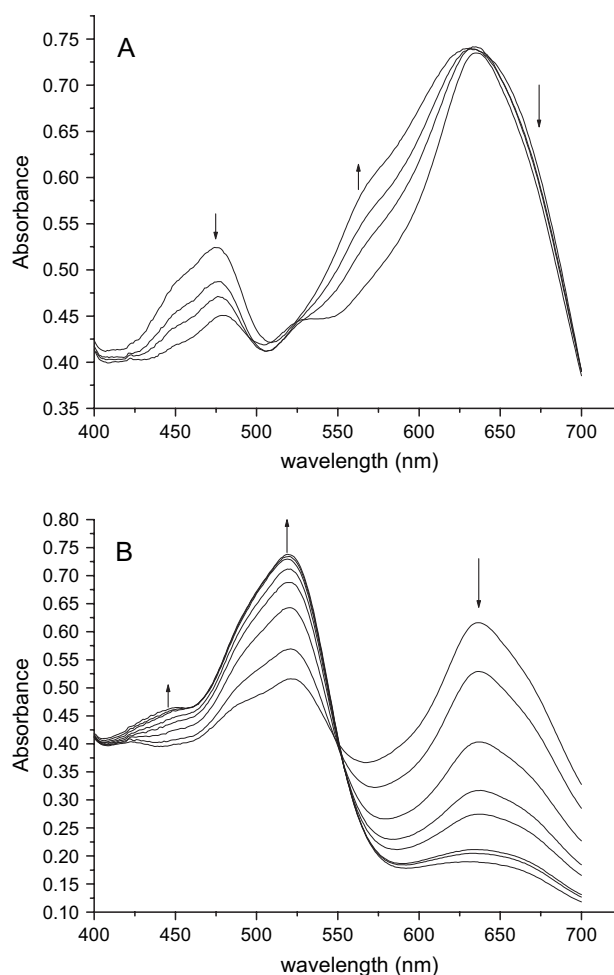
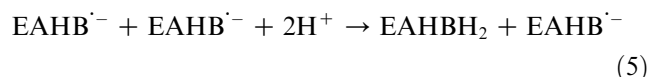


Fig. 3. Absorption spectra from deoxygenated DMSO–buffer (1:1 by volume, pH = 8.0) containing EAHB (40 μM) and NADH (1 mM) upon irradiation for (A) 0, 10, 20, 40, 80 and (B) 120, 160, 200, 240, 300, 420, 480, 600 s. The arrows indicate the direction of changes.

band of EAHB at 475 nm decreased, a new shoulder at 565 nm (belonging to the semiquinone radical anion) appeared, accompanied by two isobestic points at 524 and 643 nm (Fig. 3A), however, because the λ_{max} of EAHB^{•-} and EAHB at 632 nm are almost the same value, the absorbance above 643 nm around does not decrease obviously, when the solution color turned to yellowish green. Meanwhile, EPR measurements indicated that a signal of EAHB^{•-} can be observed. On further irradiation of the intermediate (B), another new absorption band at 519 and 450 nm (shoulder) appeared (belonging to EAHBH₂), whereas the height of the absorption band at 635 nm decreased down to near level line, with the isobestic point at 550 nm (Fig. 3B) and the appearance of the orange intermediate. EPR measurement does not detect the signal of EAHB^{•-}. These phenomena indicated that two major intermediate species were presented in the system, which are the yellowish green intermediate shown in Fig. 3A and the orange intermediate shown in Fig. 3B. When oxygen

was bubbled into the above solution after irradiation, both of these intermediates disappeared. When an oxygen-saturated solution of EAHB (40 μM) and NADH (1 mM) was irradiated, no variation of absorption spectra occurred. These suggested that both the yellowish green intermediate and the orange intermediate were the reduced forms of EAHB. Comparing our observations with previous results of hypocrellin B and its derivatives [28,29,33,34], the intermediates of yellowish green one or orange one could be EAHB $^{\cdot-}$ and hydroquinone (EAHBH $_2$), respectively. One electron transfer from donor (D) to triplet EAHB resulted in the formation of EAHB $^{\cdot-}$ (yellowish green with a $\lambda_{\text{max}} = 632$ nm, Eq. (2)). The second electron transfer (Eq. (4)) and disproportionation (Eq. (5)) resulted in the formation of EAHBH $_2$ (orange with a $\lambda_{\text{max}} = 519$ nm). EAHB $^{\cdot-}$ was very stable and decayed very slowly in deoxygenated DMSO solution where no H $^+$ ion existed. When water was a part of the reaction media such as DMSO–buffer solution, owing to the presence of H $^+$, the protonation of the anion radical (Eq. (6)) ion accelerated the second electron transfer (Eq. (7)) and disproportionation (Eq. (8)) [35].



3.3.2. Generation of superoxide anion radical species

In order to study the generation of O $_2^{\cdot-}$ from the photosensitization of EAHB, EPR spin trapping technique was used with DMPO as the spin trapper. O $_2^{\cdot-}$ was relatively stable in aprotic solvents, in which there was no free H $^+$ for the dismutation of O $_2^{\cdot-}$, so the spin trapping experiments were carried out in DMSO.

Illumination of EAHB (0.2 mM) DMSO solution containing 40 mM DMPO, an efficient O $_2^{\cdot-}$ trapper [22], in an oxygen-saturated DMSO solution with 532 nm laser at room temperature led to the generation of a strong EPR signal shown in Fig. 4. This spectrum was analyzed as a primary nitrogen triplet; each line in the triplet is split by a secondary proton; and each of these lines is further split by another proton, resulting in the observation of a 12-line EPR spectrum which is characteristic of the DMPO-OOH adduct; the g factor and the determined constants ($g = 2.0058$, $\alpha^{\text{N}} = 13.0$ G, $\alpha^{\text{H}}_{\beta} = 10.0$ G, $\alpha^{\text{H}}_{\gamma} = 1.4$ G) are in good agreement with the literature for DMPO-OOH [32]. In Fig. 5, in the presence of *p*-benzoquinone, which acted as an O $_2^{\cdot-}$

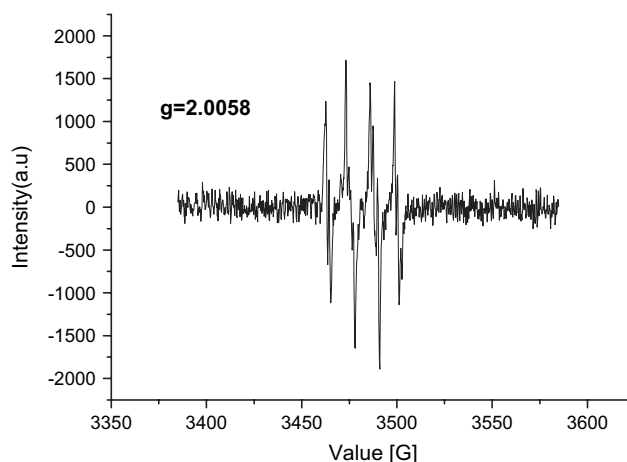


Fig. 4. The typical EPR spectrum of DMPO/OOH formed during irradiation of a DMSO solution of EAHB and DMPO. Spectrometer settings: microwave power, 1 mW; modulation amplitude, 1.012 G; time constant, 0.1024 s.

quencher [36], the EPR signals were inhibited, while in the presence of NADH which acted as an electron donor, the EPR signals were intensified, which further confirmed the generation of superoxide anion radical detected by the DMPO spin trapper. Fig. 6 and Table 1 show that the generation of superoxide anion radical in the photosensitization of EAHB was 0.76 times as effective as HB (relative quantum yields).

3.3.3. Generation of singlet oxygen species

The photooxidation of 9,10-DPA to its endoperoxide derivative by singlet oxygen O $_2$ ($^1\Delta_g$) (Scheme 2) was usually used to detect singlet oxygen generated from the photosensitizer [15]. In order to determine the quantum yield of O $_2$ ($^1\Delta_g$) generated by EAHB, we used

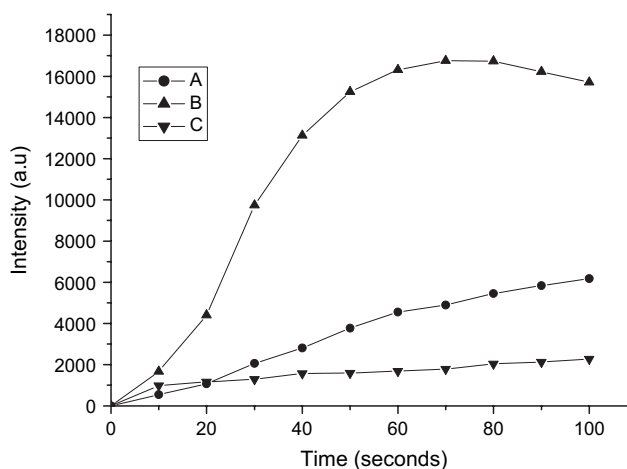


Fig. 5. Intensity of the spin adducts DMPO-OOH against duration of laser (532 nm excitation) exposure for different sensitizers in aerobic DMSO. A, EAHB (0.2 mM); B, the same as A except that NADH (5 mM) was added; C the same as B, except that PQ (0.5 mM) was added. Spectrometer settings are the same as in Fig. 2.

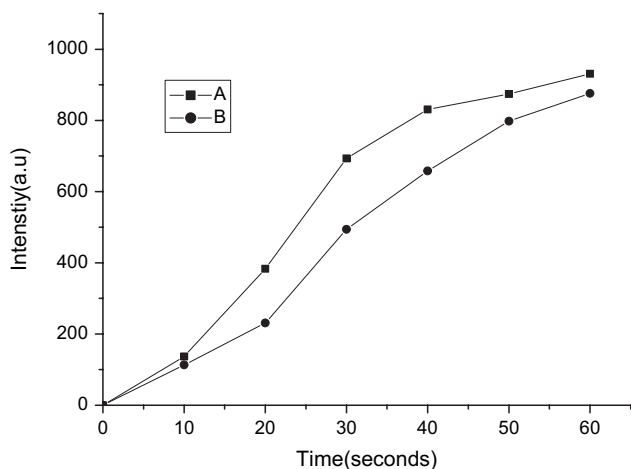


Fig. 6. The generation of superoxide anion radicals of different sensitizers in oxygen saturated DMSO solution (intensity of the spin adducts DMPO-OOH against duration of laser (532 nm excitation). A, HB (0.4 mM); B, EAHB (0.4 mM); spectrometer settings are the same as in Fig. 2.

9,10-DPA bleaching method with HB as standard in chloroform ($\Phi = 0.76$ was measured precisely with cercosporin as standard by Diwu et al. [22]).

During the measurements, the concentration of EAHB was about 0.1 mM and the absorbance at 560 nm of EAHB chloroform solution used was adjusted to be the same as that of HB chloroform solution. The rates of 9,10-DPA bleaching photosensitized by EAHB in chloroform are shown in Fig. 7. Control experiments indicated that the photosensitizer, oxygen and light were all essential for the DPA bleaching. Addition of DABCO (2 mM) inhibited DPA bleaching completely, further confirming that the bleaching of DPA resulted from the reaction of DPA with $^1\text{O}_2$ ($^1\Delta_g$) formed by EAHB photosensitization. The O_2 ($^1\Delta_g$)-generating quantum yield of EAHB in chloroform solution was estimated to be 0.15, respectively, related to HB (0.76). In addition, the O_2 ($^1\Delta_g$) generation photosensitized by EAHB in CHCl_3 solution was investigated by EPR spin trapping technique, using TEMP as a spin trapper (Scheme 3).

Illumination of EAHB (0.1 mM) containing 10 mM TEMP in an oxygen-saturated chloroform solution with 532 nm laser at room temperature led to the generation of a strong EPR spectrum (Figs. 8 and 9). The intensity of the EPR signals increased rapidly during

Table 1

The quantum yields of O_2 ($^1\Delta_g$) and the relative quantum yields of $\text{O}_2^{\cdot-}$ generated by hypocrellin B and EAHB

Compounds	Quantum yields O_2 ($^1\Delta_g$)	Relative quantum yields ($\text{O}_2^{\cdot-}$)
HB	0.76	1
EAHB	0.15	0.76

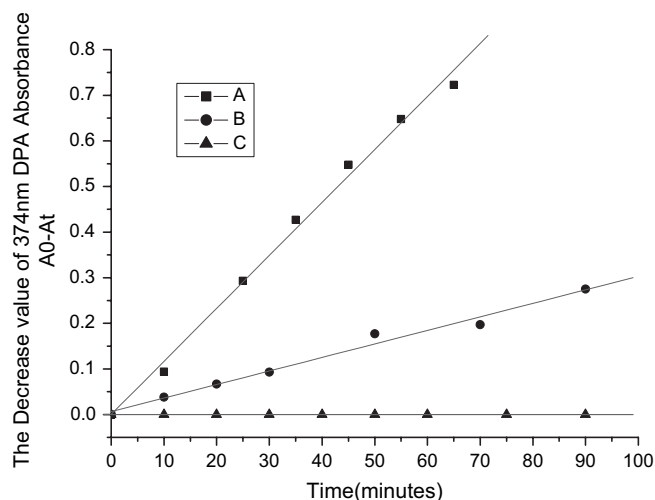
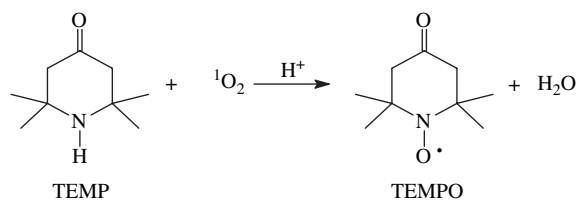


Fig. 7. Photosensitized DPA bleaching by measuring the absorbance decrease at 374 nm as a function of irradiation time in aerobic chloroform. A, HB (2×10^{-5} M); B, EAHB (2.0×10^{-5} M); C, same as B, except that DABCO (2 mM) was added.

photoillumination and decreased gradually in the dark. It depended on the concentration of EAHB and the illumination time. An EPR spectrum of three equal intensity lines, characteristic of a nitroxide radical, was observed. The g factor ($g = 2.0056$) and hyperfine splitting constant ($\alpha^N = 13.8$ G) of the EPR signals were found to be the same as those of authentic TEMPO [21], suggesting the EPR signals were due to TEMPO, generated during the illumination of the EAHB solution containing TEMP. As shown in Fig. 9, the presence of DABCO, as an O_2 ($^1\Delta_g$) scavenger, suppressed the EPR signals and Fig. 10 shows the Stern–Volmer plot for the effect of DABCO quenching, further proving that TEMPO was formed by the reaction of TEMP with O_2 ($^1\Delta_g$) generated during the irradiation of EAHB. Control experiments indicated that EAHB, oxygen and light were all essential for the formation of TEMPO. The quantum yields of O_2 ($^1\Delta_g$) generation (Fig. 9 and Table 1) were further confirmed by EPR method and HB used as the reference ($\Phi = 0.76$) to 0.15, for EAHB.

Table 1 lists the quantum yields of singlet oxygen and the relative quantum yields of superoxide anion radical generated by EAHB.



Scheme 3. The O_2 ($^1\Delta_g$) generation investigated by EPR spin trapping technique, using TEMP as a spin trapper.

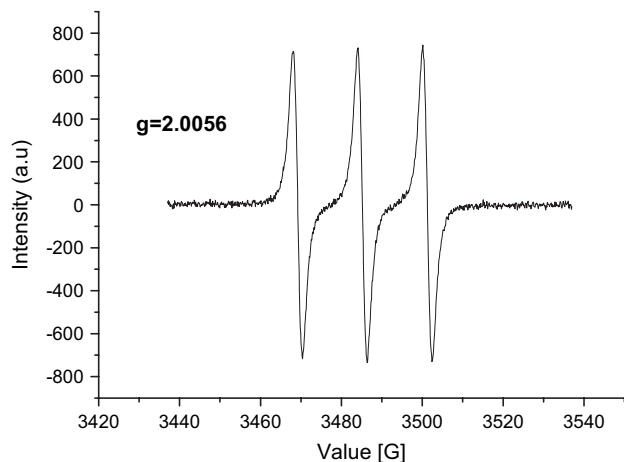


Fig. 8. The typical EPR spectrum of TEMPO generated during irradiation of chloroform solution of EAHB and TEMP. Spectrometer settings: microwave power, 5 mW; modulation amplitude, 10 G; time constant, 0.105 s.

3.4. Cell survival studies

MGC803 cancer cells were employed to study the photobiological properties of HB and EAHB. Investigation of the other cancer cells is ongoing. EAHB exhibits the same phototoxicity to its parent hypocrellin but with 4 times lower cytotoxicity than HB, with 50% cell killing at a concentration with 2 μM at a light dose of 8 J/cm^2 , and its photopotential factor was 30-fold. The data in detail are given in Table 2, which indicated EAHB as a better photodynamic therapeutic anti-cancer agent than the parent hypocrellin B.

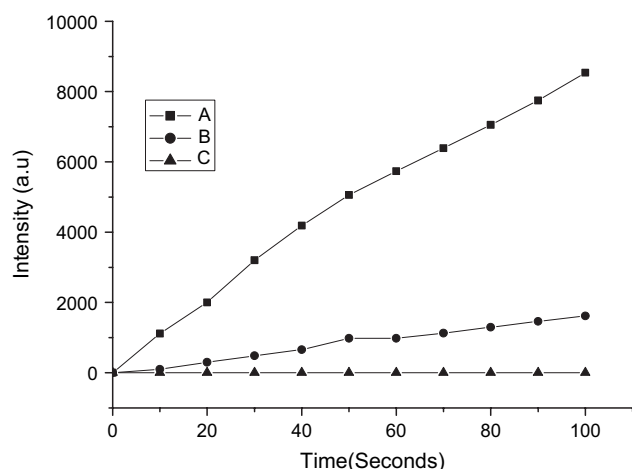


Fig. 9. The intensity of the spin adducts TEMPO against duration of laser (532 nm excitation) exposure for different sensitizers in aerobic chloroform. A, HB (0.1 mM); B, EAHB (0.1 mM); C, same as B, except that DABCO (0.5 mM) was added.

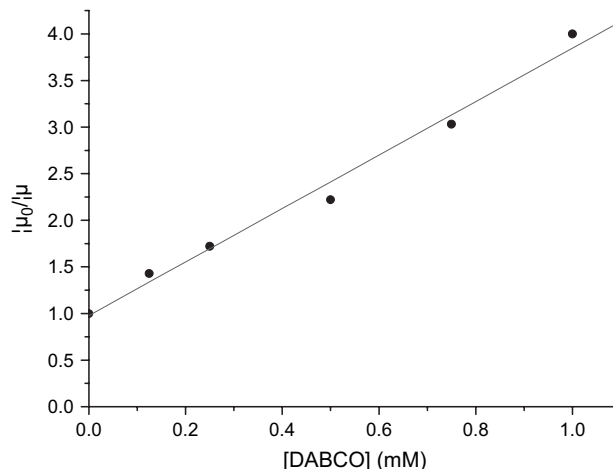


Fig. 10. Stern–Volmer plot of DABCO quenching during the singlet oxygen generation by EAHB photosensitization. Performed by adding various amount of DABCO to a series of oxygen-saturated chloroform solution (EAHB 0.1 mM).

4. Conclusions

A novel derivative of hypocrellin B, EAHB was synthesized with a simple method and its molecular structure was characterized and confirmed. In the molecular structure of EAHB, the peri-hydroxylated perylenequinone structure of the parent hypocrellin is still preserved, which may play an important role in its photodynamic action [7,37]. In the UV–vis spectra of EAHB, its absorption of red spectral region at the photodynamic window (600–900 nm) was enhanced obviously. EAHB has still strong enough generation of singlet oxygen (the quantum yields of EAHB: 0.15 in contrast with that of HB: 0.76) and superoxide anion radical (the relative quantum yields of EAHB: 0.76 in contrast with that of HB: 1). The presence of an electron donor can result in significant enhancements in the production of EAHB $^{\cdot-}$, O $_2^{\cdot-}$. We inferred that photosensitizations by EAHB involve both Type I and Type II mechanisms; in that Type I reaction is possibly the major process in the competition between both, which is similar to the photodynamic behavior of 2-butylamino-2-dimethoxy-hypocrellin B. The MGC803 cancer cell experiment displays the obvious 4-fold increasing photopotential factor more than HB but with lower cytotoxicity, although its abilities to generate singlet oxygen and superoxide anion radical are lower than those of HB. The presumable reason is that its obviously

Table 2
Results of MGC803 cancer cell-survive studies of HB and EAHB

Compounds	HB	EAHB
Cytotoxicity LD $_{50}$ (μM)	15	60
Phototoxicity LD $_{50}$ (μM)	2	2
Photopotential factor	7.5	30

enhanced absorption in the red spectral region boosts the efficiency of its killing the cancer cells during the illumination with the red laser. With the advantages mentioned above, EAHB will be a potential photodynamic therapeutic anti-cancer agent in the future.

Acknowledgements

The National Nature Science Foundation of China supported this research (No. 20172058 and 30370361).

References

- [1] Dougherty TJ, Marcus SL. Photodynamic therapy. *Eur J Cancer* 1992;28A:1734.
- [2] Dougherty TJ, Gomer CJ, Henderson BW, Jori G, Kessel D, Korbek M, et al. Photodynamic therapy. *Natl Cancer Inst* 1998; 90:889.
- [3] Foote CS. Definition of type I and type II photosensitized oxidation. *Photochem Photobiol* 1991;54:145.
- [4] Oschner M. New trends in photobiology: photophysical and photobiological process in the photodynamic therapy of tumors. *J Photochem Photobiol* 1997;39:1.
- [5] Diwu ZJ. Novel therapeutic and diagnostic applications of hypocrellins and hypericins. *Photochem Photobiol* 1993;61:131.
- [6] Hudson JB, Zhou J, Chen J, Harris L, Yip L, Towers GHN. Hypocrellin from *Hypocella bambusae*, is photo-toxic to human immunodeficiency virus. *Photochem Photobiol* 1995;61:529.
- [7] Fehr MJ, Carpenter SL, Wannemuehler Y, Petrich JW. Roles of oxygen and photoinduced acidification in the light dependent antiviral activity of hypocrellin A. *Biochemistry* 1995;34:15845.
- [8] Hudson JB, Imperial V, Haugland RP, Diwu ZJ. Antiviral activities of photoactive perylenequinones. *Photochem Photobiol* 1997;65:352.
- [9] Das K, English DS, Fehr MJ, Petrich JW. Solvent dependence on the intramolecular excited-state proton or hydrogen atom transfer in hypocrellin. *J Am Chem Soc* 1997;119:2763.
- [10] Chaloupka R, Sureau F, Kocisova E, Petrich J. Hypocrellin A photosensitization involves an intracellular pH decrease in 3T3 cells. *Photochem Photobiol* 1993;68:44.
- [11] He YY, An JY, Jiang LJ. pH effect on the spectroscopic behavior and photogeneration of semiquinone anion radical of hypocrellin B. *Dyes Pigments* 1998;41:79.
- [12] Miller GG, Brown K, Ballangrud AM, Xiao Z, John T, Lown JW. Preclinical assessment of hypocrellin B and hypocrellin B derivatives as sensitizer for photodynamic therapy of cancer: process update. *Photochem Photobiol* 1997;65:714.
- [13] Diwu ZJ, Zhang CL, Lown JW. Photosensitization with anticancer agents. 18. Perylenequinonoid pigments as potential photodynamic therapeutic agents: preparation and photodynamic properties of amino-substituted hypocrellin derivatives. *Anticancer Drug Des* 1993;8:129.
- [14] Wu T, Xu SJ, Shen JQ, Song AM, Chen S, Zhang MH, et al. New potential photodynamic therapeutic anticancer agents: synthesis and characterization of demethoxy amino-substituted hypocrellins. *Anticancer Drug Des* 2000;15:287.
- [15] Xu SJ, Chen S, Zhang MH, Tao S. Cyclohexylamino-demethoxy-hypocrellin B and its photodynamic therapy decreases human pancreatic cancer in vitro. *Biochim Biophys Acta* 2000;6:1523.
- [16] Wu T, Shen JQ, Song A, Chen S, Zhang MH, Shen T. Photodynamic action of amino substituted hypocrellin: EPR studies on the photogenerations of active oxygen and free radical species. *J Photochem Photobiol B* 2000;57:14.
- [17] Moan J, Peng Q, Evensen JF, Berg K, Western A, Rimington C. Photosensitizing efficiencies, tumor and cellular uptake of different photodynamic therapy of cancer. *Photochem Photobiol* 1987;46:713.
- [18] Zhang ZY, Zang LY, Tao NB, Wang DH. Characteristics of the initial reactions during photosensitization of hypocrellin A. *Sci Sin (B)* 1989;19:130.
- [19] Ben-Hur E, Carmichael A, Riesz P, Rosenthal I. Photochemical generation of superoxide radical and the cytotoxicity of phthalocyanines. *Int J Radiat Biol* 1985;48:837.
- [20] An JY, Hu YZ, Jiang LJ. Reactivity of semiquinone radical anion of hypocrellin A and oxygen in aprotic media. *J Photochem Photobiol B Biol* 1996;33:261.
- [21] Hadjur C, Jardon P, Jeunet A. Photosensitization by hypericin: ESR evidence for singlet oxygen and superoxide anion radicals' formation in and in vitro model. *J Photochem Photobiol B* 1994;82:1397.
- [22] Diwu ZJ, Lown JW. Photosensitization by anticancer agents. 12. Perylenequinonoid pigments a novel type of singlet oxygen sensitizer. *J Photochem Photobiol A Chem* 1992;64:273.
- [23] Hu YZ, An JY, Jing LJ. Characteristics of the reaction between semiquinone radical anion of hypocrellins A and oxygen in aprotic media. *J Photochem Photobiol A Chem* 1996;94:37.
- [24] Richter AM, Waterfield E, Jain AK, Sternberg ED, Dolphin D, Levy JG. In vitro evaluation of phototoxic properties of four structurally related benzoporphyrin derivatives. *Photochem Photobiol* 1990;52:495.
- [25] Fisher AM, Danenberg RK, Banerjee D, Bertino JR, Danenberg P, Gomer CJ. Increased photosensitivity in HL60 cells expressing wild-type p53. *Photochem Photobiol* 1997;66:265.
- [26] Diwu ZJ, Zhang CL, Lown JW. Photosensitization with anticancer agents. 15. Perylenequinonoid pigments as potential photodynamic therapeutic agents: formation of semiquinone radicals and reactive oxygen species on illumination. *Anticancer J Photochem Photobiol B* 1993;18:131.
- [27] Diwu ZJ, Zhang MH. Research on the electronic spectra of hypocrellin A and B. *Sinica Sci B* 1989;2:113.
- [28] Hu YZ, An JY, Jing LJ. Studies of the photoinduced sulfonation of hypocrellins. *J Photochem Photobiol A Chem* 1993;70:301.
- [29] Hu YZ, An JY, Jing LJ. Studies of the photoinduced sulfonation of hypocrellin A and the photodynamic action of the products. *J Photochem Photobiol B Biol* 1993;17:195.
- [30] Mayer J, Krauslklans R. Absorption spectra of the radical ions of quinones: a pulse radiolysis study. *J Chem Soc Faraday Trans* 1991;87:2943.
- [31] Finkelstein E, Rosen GM, Rauckman EJ. Spin trapping of superoxide and hydroxyle radical: practical aspects. *Arch Biochem Biophys* 1980;200:1.
- [32] Lang K, Wagnarova M, Stoka P, Dameran W. *J Photochem Photobiol A Chem* 1992;67:187.
- [33] He YY, An JY, Jiang LJ. Photodynamic action of a water-soluble hypocrellin B derivative with enhanced absorptivity in the phototherapeutic windows. I: EPR and UV-vis studies on the photogeneration of the semiquinone anion radical and hydroquinone. *J Photochem Photobiol A Chem* 1998;115:213.
- [34] Hu YZ, An JY, Jing LJ, Chen DW. Spectroscopic study on the photoreduction of hypocrellin A: generation of semiquinone radical anion and hydroquinone. *J Photochem Photobiol A Chem* 1995;89:45.
- [35] Reszka K, Lown JW. Photosensitization of anticancer agents 8, one electro reduction of motoxantrone: an ESR and spectrophotometer study. *Photochem Photobiol* 1989;50:297.
- [36] Maning LE, Kramer MK, Foote CS. Interception of $O_2^{\cdot-}$ by benzoquinone in cyanoarmatic-sensitized photooxygenation. *Tetrahedron Lett* 1984;84:2523.
- [37] Das K, English DS, Petrick JW. Deuterium isotope effect on the excited-state photophysics of hypocrellin: evidence for proton or hydrogen atom transfer. *J Phys Chem A* 1997;101:3241.